

PHOTOCATALYTIC PROPERTIES OF TiO<sub>2</sub> AND ZnO NANOPOWDERS

L. Grigorjeva<sup>1\*</sup>, J. Rikveilis<sup>1</sup>, J. Grabis<sup>2</sup>, Dz. Jankovica<sup>2</sup>,  
C. Monty<sup>3</sup>, D. Millers<sup>1</sup>, K. Smits<sup>1</sup>

<sup>1</sup>Institute of Solid State Physics, University of Latvia,  
8 Kengaraga Str., LV-1063, Riga, LATVIA

<sup>2</sup>Institute of Inorganic Chemistry, Riga Technical University  
34 Miera Str., Salaspils, LV-2169, LATVIA

<sup>3</sup>CNRS Laboratoire Procédés, Matériaux et Énergie solaire (PROMES),  
Font Romeu 66120, France

\* e-mail: lgrig@latnet.lv

Photocatalytic activity of TiO<sub>2</sub> and ZnO nanopowders is studied depending on the morphology, grain sizes and method of synthesizing. Photocatalysis of the prepared powders was evaluated by degradation of the methylene blue aqueous solution. Absorbance spectra (190–100 nm) were measured during exposure of the solution to UV light. The relationships between the photocatalytic activity and the particle size, crystal polymorph phases and grain morphology were analyzed. The photocatalytic activity of prepared TiO<sub>2</sub> nanopowders has been found to depend of the anatase-to-rutile phase ratio. Comparison is given for the photocatalytic activity of ZnO nanopowders prepared by sol-gel and solar physical vapour deposition (SPVD) methods.

**Key words:** *photocatalysis, photocatalytic activity, ZnO, TiO<sub>2</sub>, nanopowders.*

## 1. INTRODUCTION

Photocatalysis (PhC) is widely studied owing to its usefulness for oxidation of organic pollutants upon illumination with UV light [1]. Titanium dioxide is the most popular material for PhC [1–3]; however, a number of studies are devoted to such materials as ZnO, ZnWO<sub>4</sub> and some others [4–6]. Not only materials in a powder form but also TiO<sub>2</sub> or ZnO nanotubes and nanorods [4] as well as transparent TiO<sub>2</sub> films coated on quartz substrates [7] show PhC activity. The TiO<sub>2</sub>-based porous ceramic filters have been used as air cleaners under UV lamp irradiation in hospitals, schools, etc. [8]. The TiO<sub>2</sub> doping with several cations (V, W, and others) leads to a red shift of the band gap and enhanced PhC activity under visible light illumination [9, 10].

The aim of the present study was to estimate and compare the PhC activity for TiO<sub>2</sub> and ZnO powders obtained by different synthesis methods and at variable annealing temperatures and doping.

## 2. EXPERIMENTAL

### 2.1. Preparation of samples

For preparation of samples two different methods were used: solar physical vapor deposition (SPVD) [11] and sol-gel method (similar to described in [12]). In the present study,  $\text{TiO}_2$  nanoparticles were prepared by mixing 10 ml  $\text{Ti}(\text{OC}_2\text{H}_5)_4$  with 20 ml isopropyl alcohol. After stirring, 60 ml of deionized water was added under vigorous stirring, with white sediment formed. Adding  $\text{HNO}_3$  (pH  $\sim 1.5$ ) resulted in formation of white suspension in 5–10 min. The suspension was heated to 80–85 °C for 1.5–2 h until gel was formed. Then the gel was calcinated at 150 °C for 2 h. The phase composition of  $\text{TiO}_2$  samples was changed by additional calcination at 600 and 700 °C for 2 h. The powders doped with rare-earth (RE) ions were synthesized by doping RE oxides dissolved in  $\text{HNO}_3$  (1:3). For the comparative analysis of PhC activity a commercial  $\text{TiO}_2$  powder (ALDRICH anatase,  $<25$  nm, 99.7%) was used.

### 2.2. Characteristics of samples

The PhC activity of the samples was studied at 300 K. For this purpose, a methylene blue (MB) solution in distilled water (8 mg per 1 L) was prepared, and 0.05 g of catalyst was dispersed in 70 mL of the prepared MB solution. As UV light source the unfiltered radiation by a focused Hg lamp (DRK-120) was used. The radiation power at 436 nm was controlled by a THORLABS Inc. power meter PM100 and was equal to  $\sim 300$  mW/cm<sup>2</sup>. The MB solution during the PhC activity experiment was magnetically stirred under the focused lamp illumination. The probes of MB solution were tested each 10 min, centrifuged, and its optical density was measured. Figure 1 exemplifies the PhC activity by SPVD  $\text{TiO}_2$  powder. For the optical density control the 289 nm absorption peak was taken. The obtained MB degradation rate ( $D/D_0$ ) obeys the exponential law (Fig. 1, inset). For the analysis, the integral of spectra in the range 500–750 nm was used. The X-ray powder diffraction (XRD) was measured by a Bruker AXS D8 Advance diffractometer.

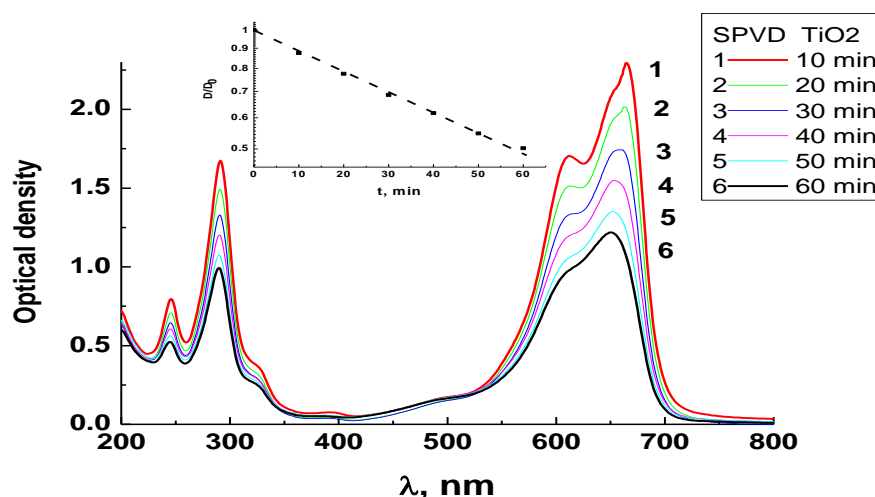


Fig. 1. MB degradation under UV light in SPVD  $\text{TiO}_2$  nanopowder.

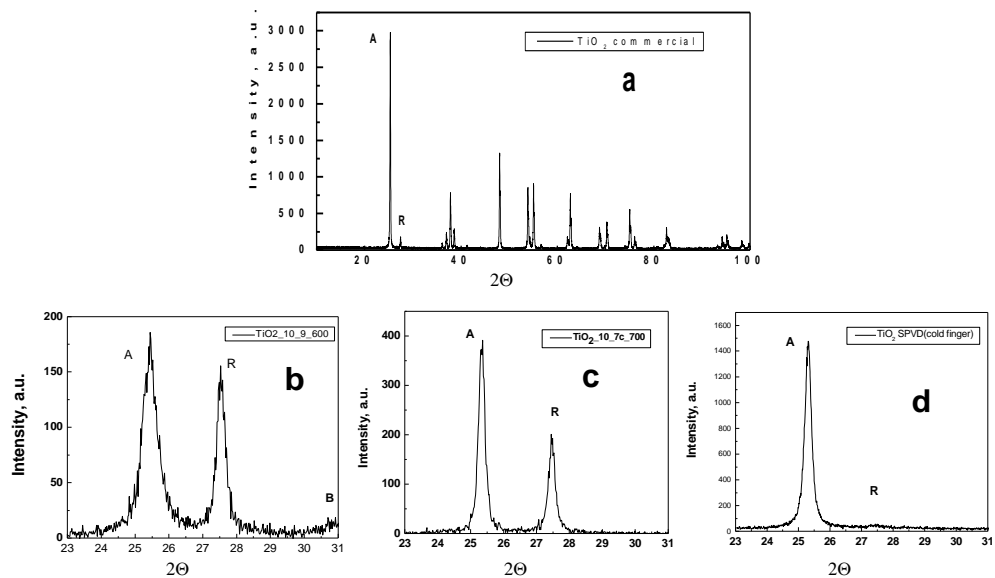


Fig. 2. XRD patterns: *a* – commercial TiO<sub>2</sub> powder; *b* – TiO<sub>2</sub>:1 at.% Eu, 600 °C; *c* – TiO<sub>2</sub>, 700 °C; *d* – TiO<sub>2</sub> SPVD; (A – anatase, R – rutile, B – brookite).

The XRD was used to determine the anatase-rutile phase composition of TiO<sub>2</sub> nanopowder. Figure 2*a–d* shows XRD patterns for the studied TiO<sub>2</sub> powders. The ratio of anatase-to-rutile weight fractions ( $X_A/X_R$ ) was calculated by the equation [13]:

$$X_R = [1 + 0.8(I_A/I_R)]^{-1},$$

where  $I_A$  and  $I_R$  are the XRD integrate line intensities at  $2\Theta = 25.4$  and  $27.5$  of the anatase and rutile phases, correspondingly.

The calculated results for  $X_A/X_R$  are shown in Table 1.

The sizes of crystallites were obtained separately for the anatase and the rutile phases from XRD peaks according to Debye–Scherr’s formula:

$$d = (0.89\lambda/\beta \cos\Theta),$$

where  $\lambda$ ,  $\beta$ ,  $\Theta$  are: the wavelength of X-ray, the full width at half maximum (FWHM) of XRD peak, and the angle of diffraction, respectively.

The BET method was used for determination of the specific surface area ( $S_{BET}$ ) taking nitrogen as adsorbent.

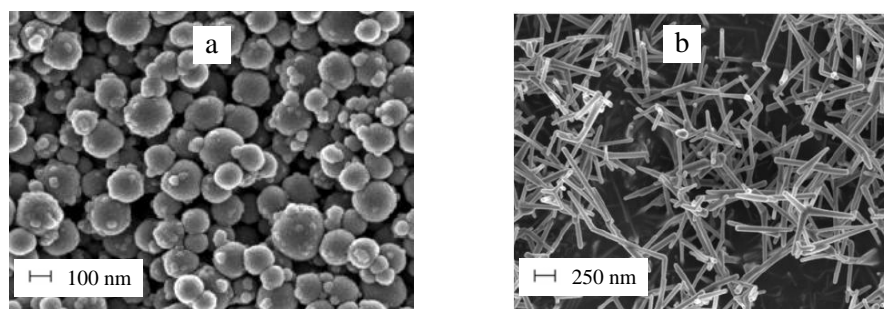


Fig. 3. SEM images of TiO<sub>2</sub> (*a*) and ZnO (*b*) nanopowders prepared by SPVD under 300 Torr air pressure.

Figure 3 displays SEM images obtained for TiO<sub>2</sub> and ZnO nanopowders prepared by SPVD under the pressure of 300 Torr.

### 3. RESULTS AND DISCUSSION

In TiO<sub>2</sub> nanopowders – undoped, doped with 1 at.% Eu, 1 at.% Sm, and doped with 1 at.% Er : 2 at.% Yb prepared by sol–gel method and calcinated at 600 °C or 700 °C – the anatase-to-rutile phase ratios and relevant grain sizes depend on the calcination temperature. It is shown that these sizes are larger for the powders calcinated at 700 °C as compared with those calcinated at 600 °C, which is explained by the growth of grains in size during calcination. The powders doped with RE ions and synthesized at the same conditions have smaller grain sizes than the undoped powders (a well-known effect for doped nanopowders [14]). In TiO<sub>2</sub> nanopowders doped with RE ions the traces of brookite phase were detected in XRD patterns; in those doped with 1 at.% Er : 2 at.% Yb the amorphous phase was detected. The presence of additional phase may affect the PhC activity, since the efficiency of generation of electron-hole pairs is different in the anatase, rutile, and brookite phases, and, therefore, in doped and undoped powders. The calcination temperature is a very important factor not only for changes in the grain size but also for those in the phase composition. Since the anatase phase is metastable [15], calcination at 600 and 700 °C leads to changes in the phase composition, with the rutile phase content increasing. In Table 1 the characteristics of TiO<sub>2</sub> powders are summarized.

Figure 4 shows the results for PhC activity of TiO<sub>2</sub> powders prepared by sol-gel method and for commercial TiO<sub>2</sub> powder. As seen in this figure, the doped with 1at.% of RE TiO<sub>2</sub> powders (samples 5, 6, for numbering see Tables 1, 2) show the same (or close) MB degradation rate. The best result was obtained for the undoped TiO<sub>2</sub> calcinated at 600 °C (sample 1), while a low rate was detected for 1 at.% Er–2 at.% Yb doped powders (samples 7, 8).

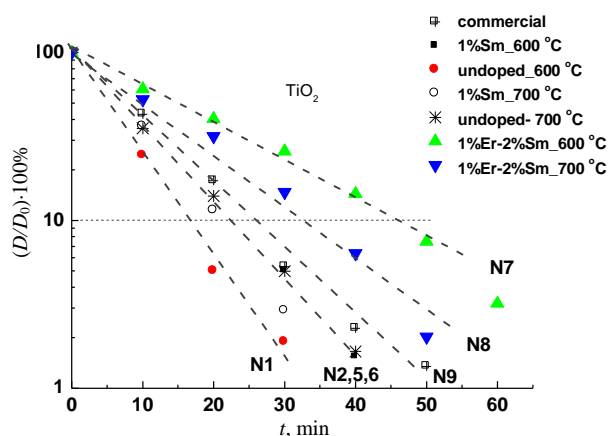


Fig. 4. PhC activity of different TiO<sub>2</sub> powders.

Table 2 shows the phase compositions ( $X_A/X_R$ ) of TiO<sub>2</sub> samples and the time during which 90% of MB concentration disappeared. This time characterizes the MB degradation rate.

Table 1

**The anatase-rutile weight fractions ( $X_A$ ,  $X_R$ ) and grain sizes ( $d_A$ ,  $d_R$ ) of TiO<sub>2</sub> powders**

| Sample No. | Sample and its calcination temperature | $S_{\text{BET}}$ , m <sup>2</sup> /g | $X_R$ | $X_A$ | $d_R$ , nm | $d_A$ , nm | Additional phase |
|------------|--|--------------------------------------|-------|-------|------------|------------|------------------|
| 1          | TiO <sub>2</sub> 600 °C                | 37.4                                 | 0.264 | 0.736 | 23         | 24         | –                |
| 2          | TiO <sub>2</sub> 700 °C                | 18.3                                 | 0.38  | 0.62  | 40         | 35         | –                |
| 3          | TiO <sub>2</sub> 1%Eu 600 °C           | 39.9                                 | 0.51  | 0.48  | 21         | 37         | Brookite         |
| 4          | TiO <sub>2</sub> 1%Eu 700 °C           | 27.3                                 | 0.63  | 0.37  | 35         | 40         | Brookite         |
| 5          | TiO <sub>2</sub> 1%Sm 600 °C           | 47                                   | 0.39  | 0.61  | 38         | 18         | Brookite         |
| 6          | TiO <sub>2</sub> 1%Sm 700 °C           | 32.9                                 | 0.432 | 0.568 | 37         | 25         | Brookite         |
| 7          | TiO <sub>2</sub> 1%Er–2%Yb 600 °C      | 40.2                                 | 0.88  | 0.18  | 17         | 7          | Amorphous        |
| 8          | TiO <sub>2</sub> 1%Er–2%Yb 700 °C      | 29.6                                 | 0.865 | 0.135 | 23         | 15         | Amorphous        |
| 9          | TiO <sub>2</sub> commercial            | 75                                   | 0.08  | 0.92  |            | 25         |                  |
| 10         | TiO <sub>2</sub> SPVD                  | ~9                                   | 0.04  | 0.96  |            | 100–150    |                  |

Table 2

**The ratio of anatase-to-rutile weight fractions ( $X_A/X_R$ ) and the time of 90% MB disappearance**

| Sample No. | Sample and its calcination temperature | $X_A/X_R$ | $t$ , min (90% MB disappear) |
|------------|--|-----------|------------------------------|
| 1          | TiO <sub>2</sub> 600 °C                | 2.79      | 16.8                         |
| 2          | TiO <sub>2</sub> 700 °C                | 1.63      | 23                           |
| 3          | TiO <sub>2</sub> 1%Eu600 °C            | 0.94      | 21                           |
| 4          | TiO <sub>2</sub> 1%Eu 700 °C           | 0.59      | 19.2                         |
| 5          | TiO <sub>2</sub> 1%Sm 600 °C           | 1.56      | 21.7                         |
| 6          | TiO <sub>2</sub> 1%Sm 700 °C           | 1.32      | 21                           |
| 7          | TiO <sub>2</sub> 1%Er–2%Yb 600 °C      | 0.2       | 42–45                        |
| 8          | TiO <sub>2</sub> 1%Er–2%Yb 700 °C      | 0.156     | 32                           |
| 9          | TiO <sub>2</sub> commercial            | 11.5      | 26                           |
| 10         | TiO <sub>2</sub> SPVD                  | 24        | 52                           |

The degradation rate dependence on the phase composition,  $S_{\text{BET}}$ , grain sizes of anatase or rutile phase, doping level, calcination temperatures and presence of additional phase have been analyzed based on the results presented in Tables 1 and 2.

It should be noted that no correlation was observed between  $S_{\text{BET}}$  and the degradation rate. Therefore, there are more important parameters that determine the PhC activity or MB degradation rate. Figure 5 shows the MB degradation rate dependence on the anatase phase ( $X_A$ ), and grain size ( $d_A$ ) for sol–gel TiO<sub>2</sub> nanopowders.

The MB degradation rate for samples 2–6 (prepared by sol–gel method) differs only slightly (90% of MB degrade in 19–22 min). Samples 7 and 8 have high RE ion concentration (1 at.% Er – 2 at.% Yb), so their MB degradation rate is considerably lower than that of the samples undoped and doped with 1 at.% Eu or 1 at.% Sm. The low MB degradation rate was detected for SPVD TiO<sub>2</sub> powder (sample 10). This powder contains ~96% of the anatase phase, while the grain size estimated from the SEM image is considerably larger (Fig. 3a) than for sol-gel TiO<sub>2</sub> powders. We suppose that the optimal grain size for high degradation rate is ~25 nm. The samples with constant phase composition but different grain sizes (10–100 nm) have to be studied additionally.

The higher MB degradation rate was obtained for sample 1 – undoped TiO<sub>2</sub> prepared by sol-gel method and calcinated at 600 °C. Our results show that doping with RE ions and calcination at 700 °C decrease the PhC activity of sol-gel TiO<sub>2</sub> powders.

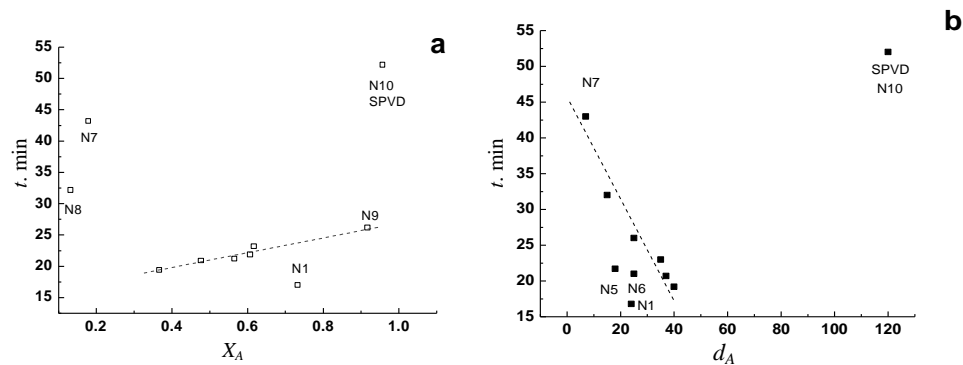


Fig. 5. MB degradation rate vs. anatase phase fraction  $X_A$  (a) and grain size  $d_A$  (b) of TiO<sub>2</sub> powders.

The SPVD method is effective for preparation of nanopowders, since these were prepared with inclusion of composites and with different dopant concentration [11]. The PhC activity of ZnO nanopowders prepared by SPVD method was studied and compared with that for TiO<sub>2</sub> powders (Fig. 6). The ZnO nanopowders doped with Ti and In were prepared from the 4.6 g ZnO : 0.2 g In<sub>2</sub>O<sub>3</sub> and 4.6 g ZnO : 0.6 g TiO<sub>2</sub> targets. Figure 6 shows low PhC activity for ZnO : In.

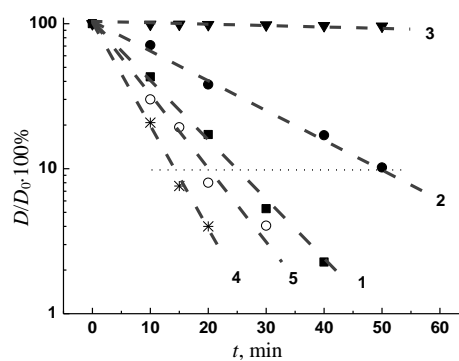


Fig. 6. PhC activity of SPVD ZnO and TiO<sub>2</sub> nanopowders: 1 – TiO<sub>2</sub> commercial; 2 – TiO<sub>2</sub>; 3 – ZnO:In; 4 – ZnO:Ti; 5 – ZnO.

The ZnO:Ti powder gives better results than the commercial TiO<sub>2</sub> and the undoped SPVD ZnO powder. Therefore, it is shown that the ZnO powders with tetrapod structure (Fig. 3b), undoped and Ti-doped are good photocatalysts. The PhC activity is low for SPVD TiO<sub>2</sub>. In [11] the grain size of anatase phase of SPVD TiO<sub>2</sub> was calculated from the XRD pattern and is very small (18 nm for powders prepared under pressure of 300 Torr). However, the grain size obtained from SEM image (Fig. 3a) is 100-150 nm, while from S<sub>BET</sub> – 120 nm. This means that the nanostructured particles are agglomerated. Moreover, small nanocrystals are coated (as seen in HRTEM images [11]). The low PhC activity of SPVD TiO<sub>2</sub> might be due to the grain surface state and the electron-hole recombination on surface defects.

#### 4. CONCLUSIONS

The most significant conclusions based on the results of study are as follows.

The methylene blue (MB) degradation in time obeys the exponential law and is straightening in semi-logarithmic coordinates  $D/D_0 = f(t)$ , where  $D$  is the optical density of MB solution in water. Experimental results show that for PhC activity of importance are the ratio of anatase-to-rutile phase and the anatase grain size. Smaller grain size does not give better PhC performance, possible due to the high concentration of surface defects and the electron-hole recombination on surface states. The doping with RE ions causes a decrease in the anatase grain size, and the PhC activity for the relevant samples is lower than for undoped powders. The PhC activity better than that for commercial TiO<sub>2</sub> powder was obtained for the undoped powder prepared by the sol-gel method. This powder has a low calcination temperature and a high weight fraction of the anatase phase.

The ZnO with a tetrapod (whiskers) morphology is found to be more efficient photocatalyst than the solgel or SPVD TiO<sub>2</sub> prepared nanopowders.

#### ACKNOWLEDGMENT

*The work was supported by LZP grant 302/2012 and SFERA Grant Agreement No. 22829.*

#### REFERENCES

1. Fujishima, A., & Zhang, X. (2006). Titanium dioxide photocatalysis: present situation and future approaches. *C.R.Chimie*, (9), 750–760.
2. Henderson, M.A. (2011). A surface science perspective on TiO<sub>2</sub> photocatalysis. *Surface Science Reports*, 66 (6/7), 185–297.
3. Rauf, M.A., Meetani M.A., & Hisaindee, S. (2011). An overview on the photocatalytic degradation of azo dyes in the presence of TiO<sub>2</sub> doped with transient metals. *Desalination*, 276, 13–27.
4. Sun, L., Zhao, D., Song, Z., Shan, Ch., Zhang, Z., Li, B., & Shen, D. (2011) Gold nanoparticles modified ZnO nanorods with improved photocatalytic activity. *J. Colloid Interface Sci.*, 363, 175–181.
5. Zhao, X., Yao, W., Wu, Y., Zhang, Sh., Yang, H., & Zhu, Y. (2006). Fabrication and photochemical properties of porous ZnWO<sub>4</sub> film. *J. of Solid State Chem.*, 179, 2562–2570.
6. Grigorjeva, L., Millers, D., Grabis, J., & Jankovica, Dz. (2011). Photoluminescence and photocatalytic activity of zinc tungsten powders. *Cent. Eur. J. Phys.*, 9 (2), 510–514.

7. Kamei, M. (2012). Sense and reproducible photocatalytic activity evaluation instrument for transparent coatings. *J. Condensed Matter Phys.*, (2), 47–49.
8. Fujishima, A., & Zhang, X. (2006). Titanium dioxide photocatalysis: present situation and future approaches. *C.R. Chimie*, 9, 750–760.
9. Kubacka, A., Fiertr, A., Martinez-Arias, A., & Fernandez-Garcia, M. (2007). Nanosized Ti–V mixed oxides: Effect of doping level in the photo-catalytic degradation of toluene using sunlight-type excitation. *Appl. Catalysis, B: Environmental*, 74, 26–33.
10. Ohtani, B. (2010). Photocatalysis A to Z – what we know and what we do not know in a scientific sense. *J. Photochem. Photobiol., C: Photochemistry Reviews*, (11), 157–178.
11. Monty, C.J.A. (2010). Characterization and properties of nanophases prepared by solar physical vapor deposition (SPVD) in the solar reactor heliotron. *Arabian J. Sci. Eng.*, 35 (1C), 93–116.
12. Xu, J., Ao, Y., Fu, D., & Yuan, Ch. (2008). A simple route for the preparation of Eu, N-codoped TiO<sub>2</sub> nanoparticles with enhanced visible light-induced photocatalytic activity. *J. Colloid Interface Sci.*, 328, 447–451.
13. Spurr R.A., & Myers, H. (1957). Quantitative analysis of anatase-rutile mixtures with an X-ray diffraction. *Anal. Chem.*, 29(5), 760–762.
14. Lojkowski, W., Gedanken, A., Grzanka, E., Opalinska, A., Strachowski, T., *et al.* (2009). Solvothermal synthesis of nanocrystalline zinc oxide doped with Mn<sup>2+</sup>, Ni<sup>2+</sup>, Co<sup>2+</sup>, and Cr<sup>3+</sup> ions. *J. Nanopart. Res.*, (11), 1991–2002.
15. Hanaor, D.A.H., & Sorrell, C.C. (2011) Review of anatase to rutile phase transformation. *J. Mater Sci.*, 46, 855–874.

## TiO<sub>2</sub> UN ZnO NANOPULVERU FOTOKATALITISKĀS ĪPAŠĪBAS

L. Grigorjeva, J. Rikveilis, J. Grabis, Dz. Jankovica,  
C. Monty, D. Millers, K. Smits

### K o p s a v i l k u m s

Darbā pētīta fotokatalīzes efektivitāte ar dažādām metodēm sintezētiem TiO<sub>2</sub> and ZnO nanopulveriem, kuriem ir atšķirīga morfoloģija un grauda izmērs. Foto katalīzes process raksturots ar metilenzilā sagraušanu ūdens šķīdumā, to apstarojot ar UV gaismu. Analizēta fotokatalīzes efektivitātes atkarība no grauda izmēra, nanokristālu graudu morfoloģijas, TiO<sub>2</sub> nanopulveru anatasa-rutīla fāžu svara attiecībām. Parādīts, ka fotokatalītiskā efektivitāte ir atšķirīga TiO<sub>2</sub> nanopulveriem sintezētiem ar dažādām metodēm: sola–gēla un tvaicēšanu–kondensēšanu saules reaktorā. Salīdzināta fotokatalīzes efektivitāte ZnO un TiO<sub>2</sub> nanopulveriem un secināts, ka ZnO nanopulveri ar tetrapodu morfoloģiju ir labs fotokatalizators.

03.04.2013.